PAPER #603

THE HYDROELASTIC BEHAVIOUR OF SALTER'S DUCK IN WAVES

C.A.L. Conceição, Ph.D.*
M.A.S. Neves, Ph.D.*

ABSTRACT

This work discusses the hydroelastic behaviour of a Salter's Duck wave energy device. An important feature of such a device is its unsymmetric underwater part which is responsible for the coupling of the equations relative to the symmetric and antisymmetric motions. A numerical application focusing an idealized Salter's Duck is used to illustrate the present approach.

* Senior Lecturer, Naval Architecture Dept., COPPE - Universidade Federal do Rio de Janeiro - R.J., BRAZIL

NOTATION

$C_o(x)$	Distributed torsional stiffness ($C_o(x) = G\, I_t(x)$)
E	Young's Modulus
G	Shear Modulus
$I_{sc}(x)$	Moment of inertia per unit length about the longitudinal axis through S
$I_t(x)$	Polar moment of area about C'
$I_y(x)$	Second moment of area about the principal axis O_z
$I_{yy}(x)$	Moment of inertia per unit length about axis parallel to O_y through C
$I_{yz}(x)$	Product of inertia per unit length about axes parallel to O_y and O_z, both passing through C
$I_z(x)$	Second moment of area about the principal axis O_y
$I_{zz}(x)$	Moment of inertia per unit length about axis parallel to O_z through C
$K(x,t)$	External rolling moment per unit length about C
$K_{y,z}AG(x)$	Shear rigidity related to O_y and O_z - direction respectively
L	Length of the beam
ℓ	Characteristic length
$M_{y,z}(x,t)$	Bending moments about axes parallel to O_z and O_y respectively
$M_{y_r,z_r}(x)$	Modal bending moments about O_z and O_y - direction respectively corresponding to the r^{th} principal mode
O_{xyz}	System of equilibrium axes situated at the aft end of the Duck

$p_r(t)$	r^{th} principal coordinate of the dry-hull
r,s	Modal indices
S	Sectional shear centre
$T(x,t)$	Twisting moment
t	Time
$V_{y,z}(x,t)$	Shear forces in the directions O_y and O_z respectively
$V_{y_r,z_r}(x)$	Modal shear force in the O_y and O_z - direction respectively, corresponding to the r^{th} principal mode
$v(x,t)$	Deflection at S in the O_y - direction
$v_r(x)$	Deflection in the O_y - direction at S in the r^{th} principal mode
$w(x,t)$	Deflection at S in the O_z - direction
$w_r(x)$	Deflection in the O_z - direction at S in the r^{th} principal mode
x	Coordinate in the O_{xyz} - system
$\bar{x}$	Distance of LCG from aft end of the hull
$y(x,t)$	External force per unit length in the O_y - direction applied at C
y	Coordinate in the O_{xyz} - system
$\bar{y}(x)$	$\bar{y}(x) = y_c(x) - y_{sc}(x)$
$Z(x,t)$	External force per unit length in the O_z - direction applied at C
z	Cordinate in the O_{xyz} - system
$\gamma_{y,z}(x,t)$	Shear deformation in the O_y and O_z - direction respectively
$\theta(x,t)$	Slope of the elastic curve of the beam in the plane O_{xz}

λ	Wave - length
$\mu(x)$	Mass per unit length
$\phi(x,t)$	Angular displacement about longitudinal axis
$\phi_r(x)$	Twisting deflection in the r^{th} principal mode
χ	Heading angle
$\Psi(x,t)$	Slope of the elastic curve of the beam in the plane O_{xy}
ω	Wave frequency
ω_e	Wave-encounter frequency
ω_r	r^{th} natural frequency of the dry hull

I - INTRODUCTION

In the wake of the oil crisis that hit the world in the early 70's, sea waves started been looked more enthusiastically as a possible alternative supplier of energy. Since those days, several devices have been designed for extracting wave-energy. The Salter's Duck cam is one of them which showed a promising performance. Its general features and mechanical characteristics have already been described rather extensively by its inventor and other authors (Refs. |1| ~ |5|). For the Naval Architects, the Duck's behaviour in waves brought about an interesting problem which arises from its unsymmetric cross-sections. This unsymmetry is responsible for the coupling of the horizontal with the vertical motions which, in general, does not occur when conventional ships are concerned.

There are some few papers which deal with the rigid body response of the Duck (eg, Refs. |2|, |3| & |4|). This work intends to press the problem a little further by introducing the effects of the flexibility of each segment of the Salter's Cam upon its response to wave excitation.

II - EQUATIONS OF MOTION OF A SALTER'S DUCK SEGMENT

Considering the slice of a Salter's Duck beam floating in waves - Figure I, the following equations of motion can be formed:

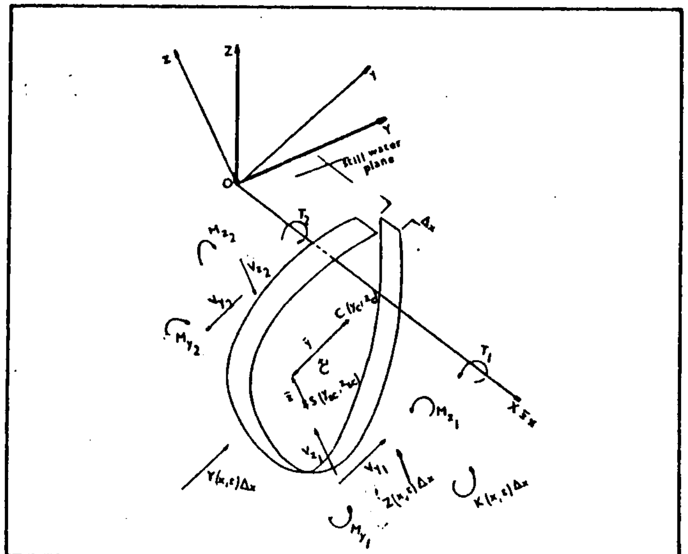

Figure I : Slice of an unsymmetric section. C - centre of mass with coordinates (y_c, z_c). S - centre of shear with coordinates (y_{sc}, z_{sc}). C' - centroid. The figure shows the sign conventions for the bending moments, shear forces and twisting moment.

$$\mu(x)\ \{\ddot{w}(x,t) + \bar{y}(x)\ \ddot{\phi}(x,t)\} = V'_z(x,t) + Z(x,t)$$

$$\mu(x)\ \{\ddot{v}(x,t) - \bar{z}(x)\ \ddot{\phi}(x,t)\} = V'_y(x,t) + Y(x,t)$$

$$I_{sc}(x)\ \ddot{\phi}(x,t) - \mu(x)\ \bar{z}(x)\ \ddot{v}(x,t) + \mu(x)\ \bar{y}(x)\ \ddot{w}(x,t) = T'(x,t) - \bar{z}(x)\ Y(x,t) + \bar{y}(x)\ Z(x,t) + K(x,t)$$

$$I_{yy}(x)\ \ddot{\theta}(x,t) - I_{yz}(x)\ \ddot{\Psi}(x,t) = -M'_z(x,t) - V_z(x,t)$$

$$I_{zz}(x)\ \ddot{\Psi}(x,t) - I_{yz}(x)\ \ddot{\theta}(x,t) = M'_y(x,t) + V_y(x,t)$$

According to elementary beam theory, if O_z and O_y are principal directions of the structural area, the expressions relating shear forces, bending moments and twisting moment to the distortions of the beam may be written as:

$$V_z(x,t) = K_z AG(x)\{w'(x,t) + \theta(x,t)\} = K_z AG(x)\ \gamma_z(x,t) + K_z AG(x)\ \alpha_z(x)\ \dot{\gamma}_z(x,t)$$

$$V_y(x,t) = K_y AG(x)\{v'(x,t) - \Psi(x,t)\} = K_y AG(x)\ \gamma_y(x,t) + K_y AG(x)\ \alpha_y(x)\ \dot{\gamma}_y(x,t)$$

$$M_z(x,t) = -EI_y(x)\ \theta'(x,t) - EI_y(x)\ \beta_z(x)\ \dot{\theta}'(x,t)$$

$$M_y(x,t) = EI_z(x)\ \Psi'(x,t) + EI_z(x)\ \beta_y(x)\ \dot{\Psi}'(x,t)$$

$$T(x,t) = C_o(x)\ \phi'(x,t) - \{C_1(x)\ \phi''(x,t)\}' + \Gamma(x)\ \dot{\phi}'(x,t)$$

The factors $\alpha_{y,z}(x)$, $\beta_{y,z}(x)$ and $\Gamma(x)$ provide a way of taking into consideration the internal damping of the structure which occurs during bending, shear and twisting respectively. Such an approach has been developed by Kumai (Ref. |6|) and an interesting review on these factors has been published by Betts et al. (Ref. |7|). The factors $K_{y,z}$ are dependent on the shape of the cross-section. They are introduced to account for the fact that the shear stresses are not uniformly distributed over the cross-section. The effect of warping was included in the twisting moment equation following the approach proposed by Timoshenko (Ref. |8|). The warping coefficient - $C_1(x)$ can be calculated by using the procedures given by Haslum and Tonnessen (Ref. |9|).

The coupled equations of motion can be solved by means of Modal Analysis using a set of principal coordinates corresponding to the characteristic functions and frequencies obtained not including fluid actions - the "Dry"-Modes (eg, Ref. |10|).

After some trivial but rather tedious algebraic treatment, integrating the equations of motion over the length of the beam, application of some convenient orthogonality conditions and some special attention to introduce rigid body motions into the same set of equations, in order to reconcile the distortional and the bodily displacements, the generalized equations of motion may be defined as (for details, see Ref. |11|):

$$a_{00}\ddot{p}_0(t) + a_{40}\ddot{p}_4(t) = \int_0^L Z(x,t)\, dx$$

$$a_{11}\ddot{p}_1(t) + a_{41}\ddot{p}_4(t) = \int_0^L Z(x,t)\, (1 - \frac{x}{\bar{x}})\, dx$$

$$a_{22}\ddot{p}_2(t) + a_{42}\ddot{p}_4(t) = \int_0^L Y(x,t)\, dx$$

$$a_{33}\ddot{p}_3(t) + a_{43}\ddot{p}_4(t) = \int_0^L Y(x,t)\, (1 - \frac{x}{\bar{x}})\, dx$$

$$a_{04}\ddot{p}_0(t) + a_{14}\ddot{p}_1(t) + a_{24}\ddot{p}_2(t) + a_{34}\ddot{p}_3(t) + a_{44}\ddot{p}_4(t) =$$

$$\int_0^L \{Z(x,t)\, y_c(x) - Y(x,t)\, z_c(x) + K(x,t)\}\, dx$$

$$a_{ss}\ddot{p}_s(t) + \sum_{r=5}^{\infty} (\alpha_{rs} + \beta_{rs} + \Gamma_{rs})\, \dot{p}_r(t) + \omega_s^2\, a_{ss}\, p_s(t) =$$

$$\int_0^L \{Z(x,t)\,|w_s(x) + \bar{y}(x)\, \phi_s(x)| + Y(x,t)\,|v_s(x) + \bar{z}(x)\, \phi_s(x)| + K(x,t)\, \phi_s(x)\}\, dx, \quad \text{if } s \geq 5$$

Where:

$$a_{04} = \int_0^L \mu(x)\, y_c(x)\, dx = a_{40}$$

$$a_{14} = \int_0^L \mu(x)\, (1 - \frac{x}{\bar{x}})\, y_c(x)\, dx = a_{41}$$

$$a_{24} = -\int_0^L \mu(x)\, z_c(x)\, dx = a_{42}$$

$$a_{34} = -\int_0^L \mu(x)\, (1 - \frac{x}{\bar{x}})\, z_c(x)\, dx = a_{43}$$

if, $w_0(x) = 1{,}0; \quad v_0(x) = 0 = \phi_0(x); \quad w_1(x) = (1 - \frac{x}{x}),$

$v_1(x) = 0 = \phi_1(x); \quad v_2(x) = 1.0, \quad w_2(x) = 0 = \phi_2(x);$

$v_3(x) = (1 - \frac{x}{x}), \quad w_3(x) = 0 = \phi_3(x); \quad \phi_4(x) = 1.0,$

$w_4(x) = y_{sc}(x), \quad v_4(x) = - z_{sc}(x).$

In these generalized equations of motion the following definitions are applied:

$$a_{rs}\,\delta_{rs} = \int_0^L \{\mu(x)\, w_r(x)\, w_s(x) + \mu(x)\, v_r(x)\, v_s(x) + I_{yy}(x)\, \theta_r(x)\, \theta_s(x) + I_{zz}(x)\, \Psi_r(x)\, \Psi_s(x) + I_{sc}(x)\, \phi_r(x)\, \phi_s(x) - \mu(x)\, \bar{z}(x) |\phi_r(x) v_s(x) + \phi_s(x)\, v_r(x)| + \mu(x)\, \bar{y}(x)\, |\phi_r(x)\, w_s(x) + \phi_s(x)\, w_r(x)| - I_{yz}(x)\, |\theta_r(x)\, \Psi_s(x) + \theta_s(x)\, \Psi_r(x)\} \, dx$$

$$\delta_{rs} = \text{Kronecker-delta function} = \begin{cases} 0, & \text{if } r \neq s \\ 1, & \text{if } r = s \end{cases}$$

$$\alpha_{rs} = \int_0^L \{\alpha_z(x)\, K_z\, AG(x)\, \gamma_{zr}(x)\, \gamma_{zs}(x) + \alpha_y(x)\, K_y\, AG(x)\, \gamma_{yr}(x)\, \gamma_{ys}(x)\} \, dx$$

$$\beta_{rs} = \int_0^L \{\beta_z(x)\, EI_y(x)\, \theta'_r(x)\, \theta'_s(x) + \beta_y(x)\, EI_z(x)\, \Psi'_r(x)\, \Psi'_s(x)\} \, dx$$

and

$$\Gamma_{rs} = \int_0^L \Gamma(x)\, \phi'_r(x)\, \phi'_s(x)\, dx$$

The fluid actions can be taken into consideration by employing the concept of "Strip-Theory" where the two-dimensional hydrodynamic properties of the Salter's unsymmetric cross-sections are calculated by a conformal transformation technique as given by Ref. |12|.

Substituting the principal coordinates which appear in the equations of motion by their expressions associated with sinusoidal responses - $p_r(t) = p_r e^{-i\omega_e t}$, and the fluid actions by their generalized definitions as derived in Ref. |11|, the set of equations of motion may be expressed in matrix formulation as:

$$\left\{ - \omega_e^2\, (\underset{\sim}{a} + \underset{\sim}{A}) + (\underset{\sim}{c} + \underset{\sim}{C}) - i\omega_e\, (\underset{\sim}{b} + \underset{\sim}{B}) \right\} \underset{\sim}{p} = \underset{\sim}{\Xi}$$

Where:

$\underset{\sim}{A}$ - added mass matrix

$\underset{\sim}{B}$ - damping coefficient matrix

$\underset{\sim}{C}$ - fluid restoration matrix

$\underset{\sim}{a}$ - generalized mass matrix

$\underset{\sim}{b}$ - generalized structural damping matrix

$\underset{\sim}{p}$ - principal coordinate vector

$\underset{\sim}{\Xi}$ - generalized wave excitation vector

III - NUMERICAL APPLICATION

To illustrate the present approach, a numerical example was carried out using an idealized structure of a Salter's Duck-like beam. The cross-section of this structure is shown in Figure II and all relevant data are presented in Figure III and Table I.

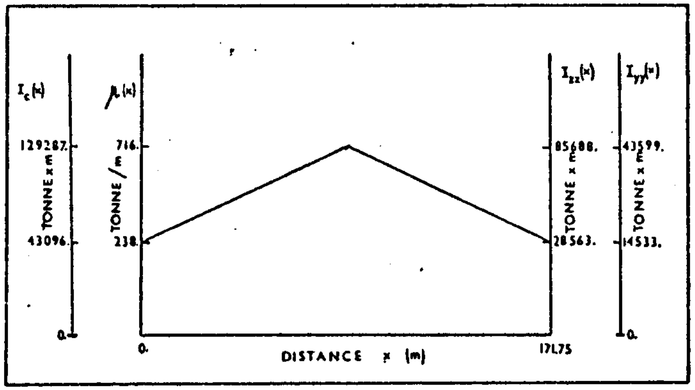

Figure II. : Distribution of $\mu(x)$, $I_c(x)$, $I_{zz}(x)$ and $I_{yy}(x)$ along the idealized Salter's Duck. $k_z AG(x) = 1.39 m^2 = const.; k_y AG(x) = 1.39 m^2 = const.$

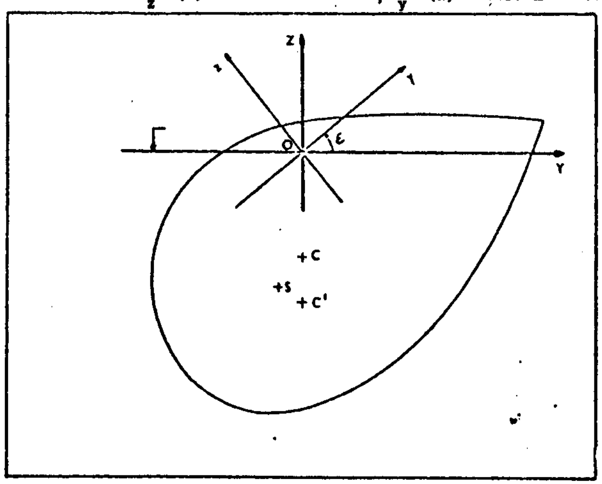

Figure III: Idealized Salter's Duck cross-section. C - centre of mass. C' - centre of buoyancy. S - centre of shear.

Table II shows the natural frequencies and number of modes corresponding to the first eight flexible modes of the "dry"-structure. Figure IV(a)-(ℓ) complements this table showing the characteristic functions associated with the two lowest flexible modes of the Salter's Duck.

Y_c	0.0
Z_c	- 5.00
$Y_{c'}$	0.0
$Z_{c'}$	- 9.50
Y_{sc}	- 0.248
Z_{sc}	- 8.971
(m)	171.75
immersed area (m^2)	465.659
ε (deg.)	32.712
EI_y ($KN \cdot m^2$)	17554.538 x 10^6
EI_z ($KN \cdot m^2$)	34500.855 x 10^6
$k_z AG = k_y AG$ (KN)	46.102 x 10^6
C_0 ($KN \cdot m^2$)	162.327 x 10^8
C_1 ($KN \cdot m^4$)	warping not included

OFFSET POINTS		OFFSET POINTS (cont'd)	
Z	Y	Z	Y
0.0	-7.05	1.00	-1.50
-0.90	-8.33	-20.60	1.00
-2.50	-10.25	-19.75	3.30
-4.50	-11.70	-18.55	5.55
-6.80	-12.95	-17.10	7.30
-9.00	-13.50	-15.20	9.05
-11.50	-13.60	-13.25	10.55
-14.10	-13.20	-11.00	11.80
-16.30	-12.02	-8.80	12.80
-18.20	-10.70	-6.60	13.95
-20.65	-6.40	-1.75	15.55
-21.10	-3.95	0.0	16.00

Table I : Idealized Salter's Duck relevant data and off-set.

MODE	NAT. FREQ. (rad/s)	Number of nodes		
		B_z	B_y	T
5	4.472	2	2	2
6	5.744	2	2	2
7	9.829	3	3	1
8	10.140	3	3	1
9	11.685	1	3	1
10	15.734	4	4	2
11	17.381	4	4	2
12	18.893	2	4	2

Table II : Dry-analysis of the idealized Salter's Duck. The dominant motions are underlined in each mode.

IDEALIZED SALTER'S DUCK-DRY HULL MODE 5 NAT. FREQ. = 4.480 RAD/SEC

Figure IV (a): Variation of $w_5(x)$.

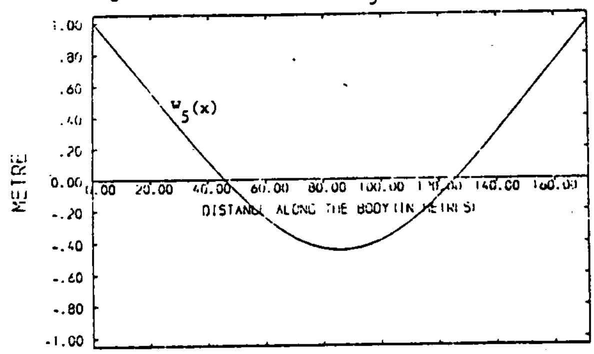

UNSYMMETRIC BODY NO WARPING,SHEAR IN ,ROTARY IN

OZ-DIR. DEFLECTION

IDEALIZED SALTER'S DUCK-DRY HULL MODE 5 NAT. FREQ. = 4.480 RAD/SEC

Figure IV(b): Variation of $v_5(x)$

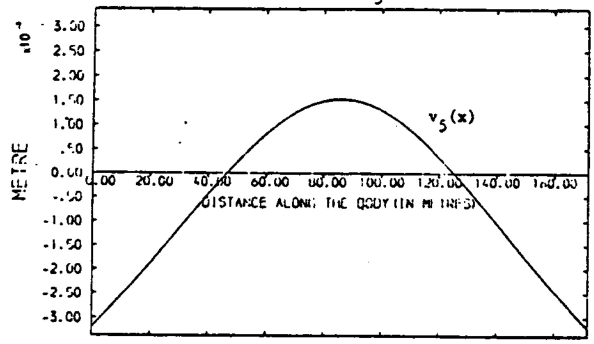

UNSYMMETRIC BODY NO WARPING,SHEAR IN ,ROTARY IN

OY-DIR. DEFLECTION

IDEALIZED SALTER'S DUCK-DRY HULL MODE 5 NAT. FREQ. = 4.480 RAD/SEC

Figure IV(c): Variations of $M_{z_5}(x)$ and $M_{y_5}(x)$.

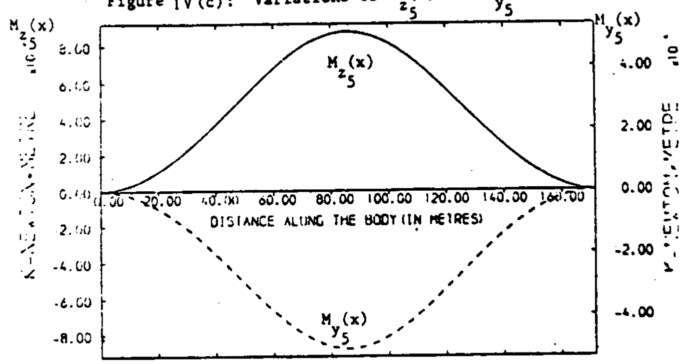

UNSYMMETRIC BODY NO WARPING,SHEAR IN ,ROTARY IN

OZ-DIR. AND OY-DIR. BENDING MOMENTS

IDEALIZED SALTER'S DUCK-DRY HULL MODE 5 NAT. FREQ. = 4.480 RAD/SEC

Figure IV(d): Variation of $\phi_5(x)$.

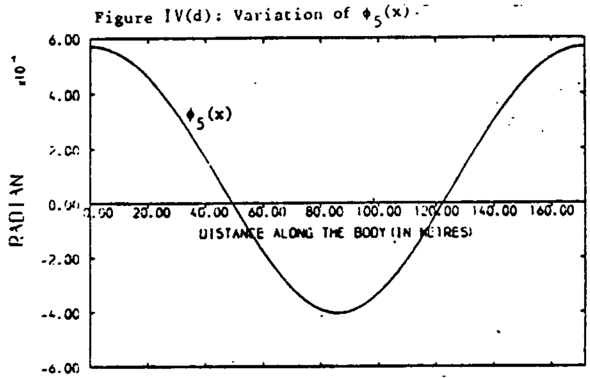

UNSYMMETRIC BODY NO WARPING,SHEAR IN ,ROTARY IN

TWIST DEFLECTION

IDEALIZED SALTER'S DUCK-DRY HULL MODE 5 NAT. FREQ. = 4.480 RAD/SEC

Figure IV(e): Variations of $V_{z_5}(x)$ and $V_{y_5}(x)$.

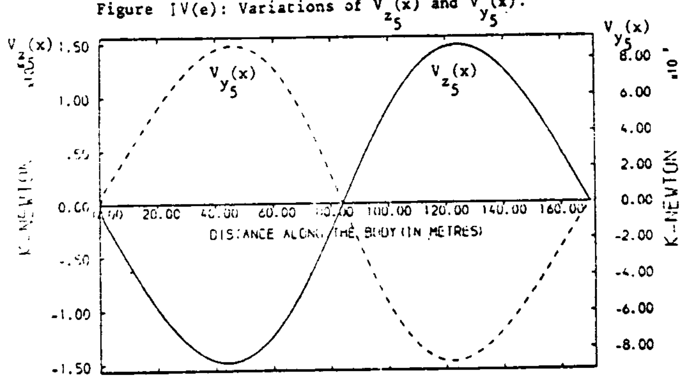

UNSYMMETRIC BODY NO WARPING,SHEAR IN ,ROTARY IN

OZ-DIR. AND OY-DIR. SHEAR FORCES

IDEALIZED SALTER'S DUCK-DRY HULL MODE 5 NAT. FREQ. = 4.480 RAD/SEC

Figure IV(f): Variation of $T_5(x)$.

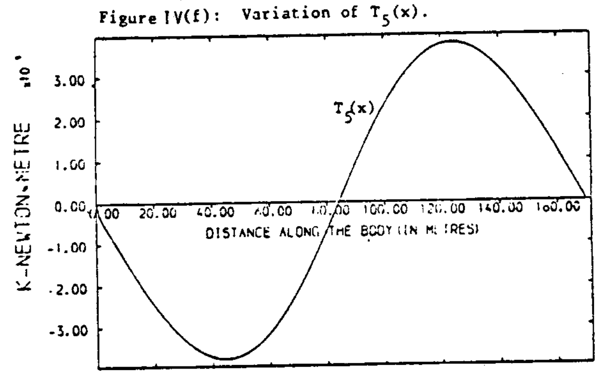

UNSYMMETRIC BODY NO WARPING,SHEAR IN ,ROTARY IN

TWIST MOMENT

IDEALIZED SALTER'S DUCK-DRY HULL MODE 6 NAT. FREQ. = 5.751 RAD/SEC

Figure IV(g): Variation of $w_6(x)$.

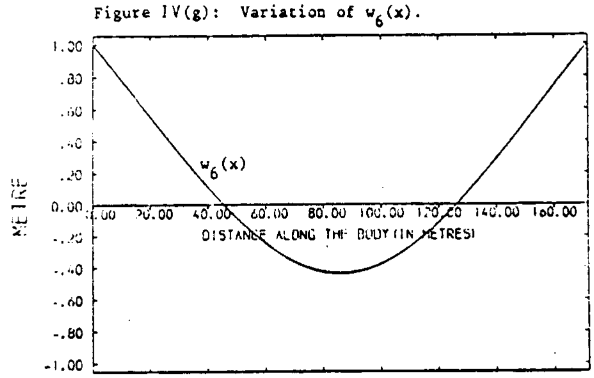

UNSYMMETRIC BODY NO WARPING,SHEAR IN ,ROTARY IN

OZ-DIR. DEFLECTION

IDEALIZED SALTER'S DUCK-DRY HULL MODE 6 NAT. FREQ. = 5.751 RAD/SEC

Figure IV(h): Variation of $v_6(x)$.

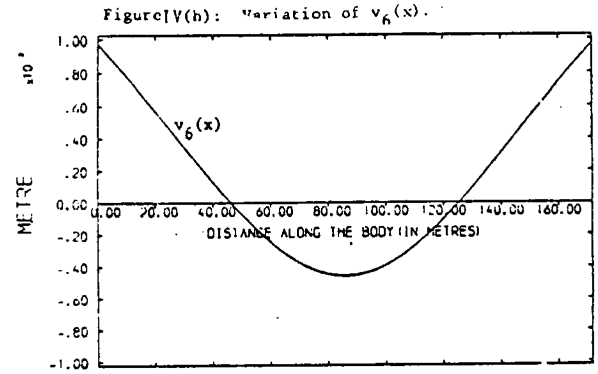

UNSYMMETRIC BODY NO WARPING,SHEAR IN ,ROTARY IN

OY-DIR. DEFLECTION

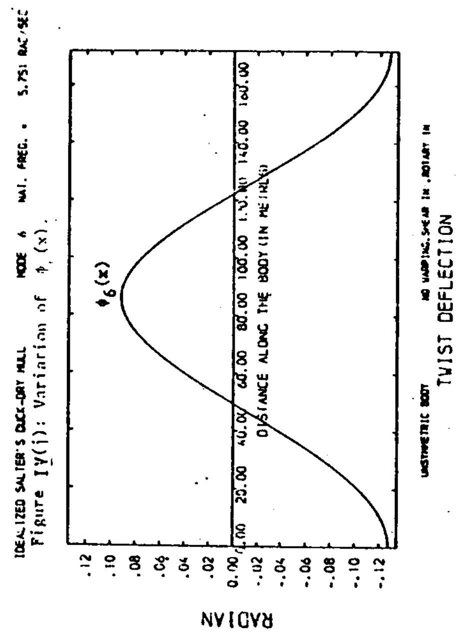

Figure IV(j): Variation of $\phi_6(x)$.

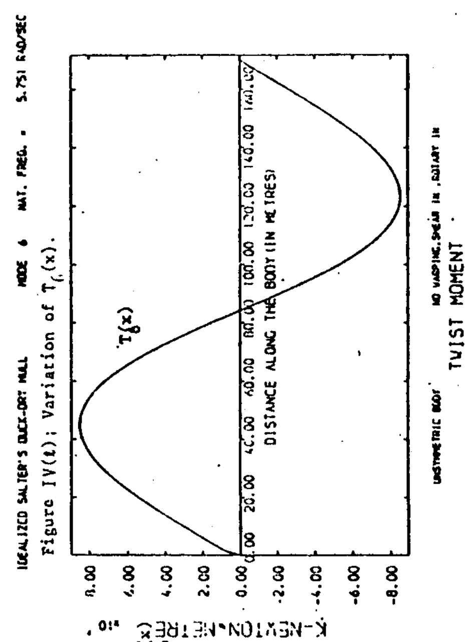

Figure IV(ℓ): Variation of $T_6(x)$.

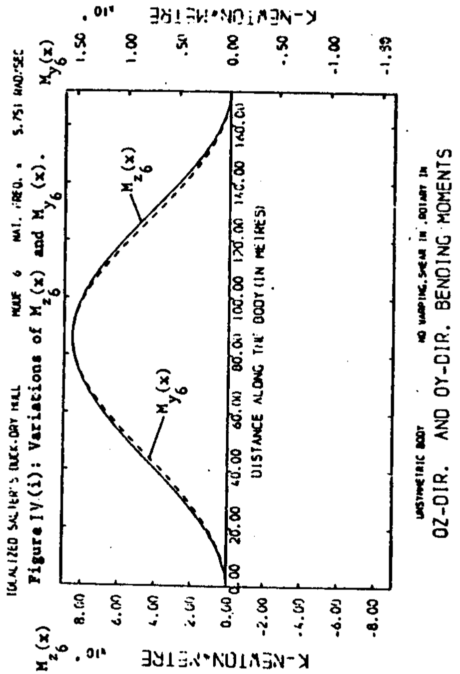

Figure IV(i): Variations of $M_{z_6}(x)$ and $M_{y_6}(x)$.

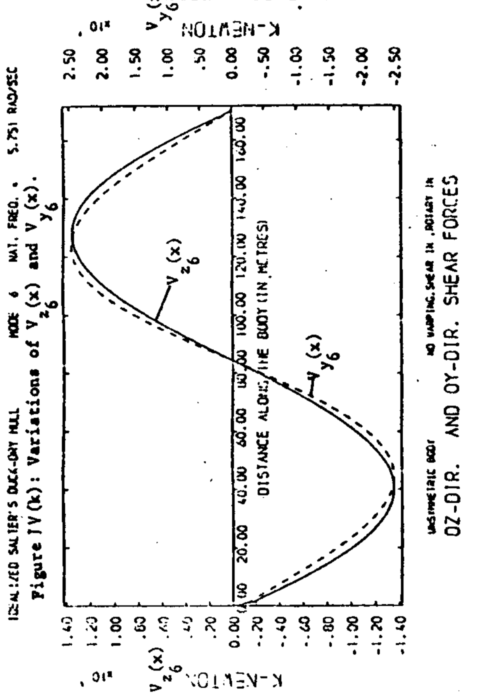

Figure IV(k): Variations of $V_{z_6}(x)$ and $V_{y_6}(x)$.

The secctional hydrodynamic coefficients calculated by means of conformal transformation technique for a one-to-ten scaled model of the Salter's Duck are shown in Figure V in a dimensional form. In these graphs, predictions using Frank Close-Fit method also appear as a matter of comparison.

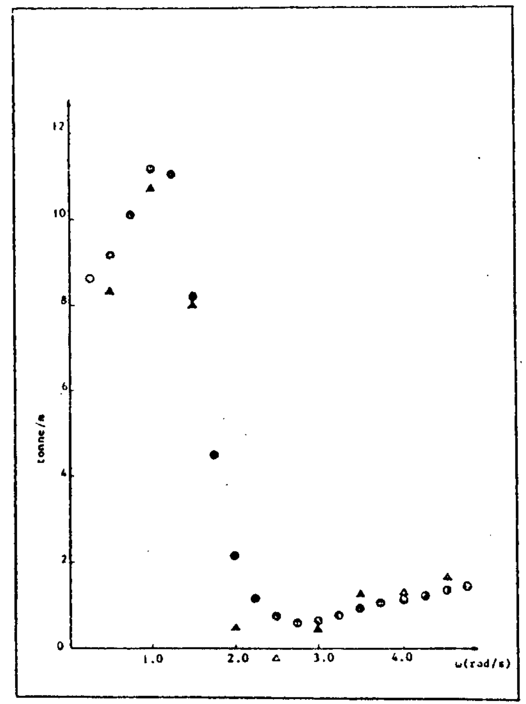

Figure V(a): Sway - Sway Added Mass.

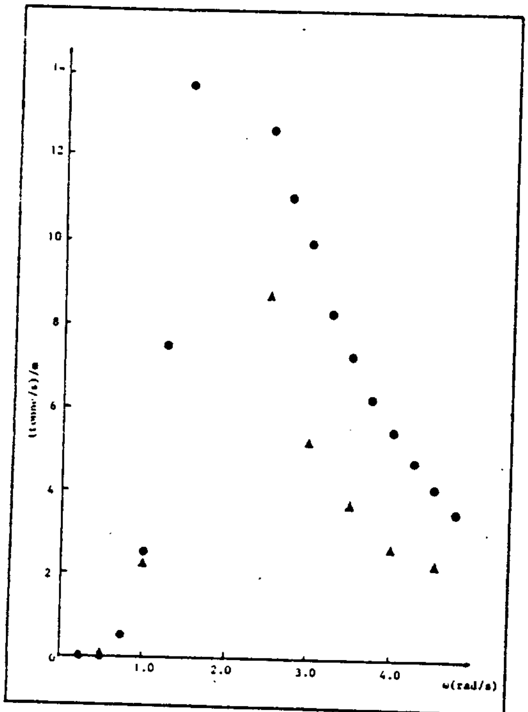

Figure V(b): Sway - Sway Damping.

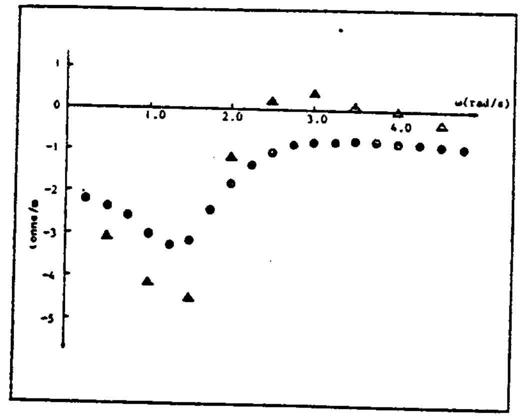

Figure V(c): Sway (Heave) - Heave (Sway) Added Mass.

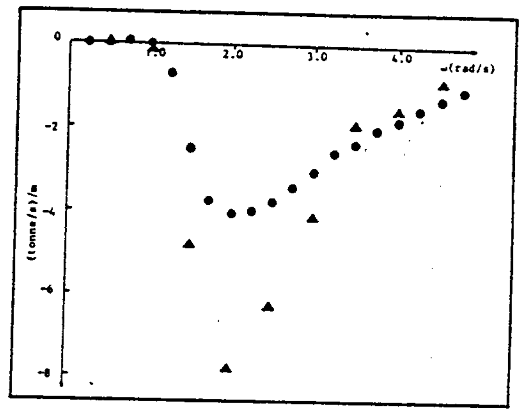

Figure V(d): Sway (Heave) - Heave (Sway) Damping.

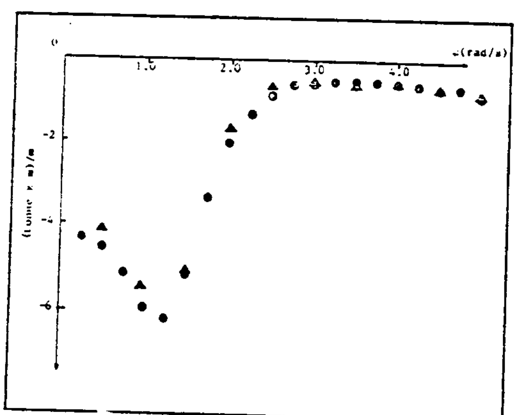

Figure V(e): Sway (Roll) - Roll (Sway) Added Mass.

Figure V(f): Sway (Roll) - Roll (Sway) Damping.

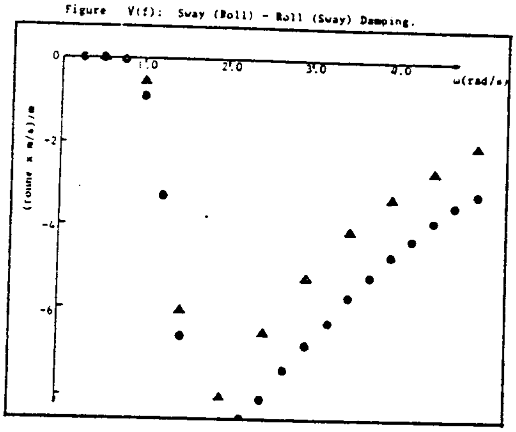

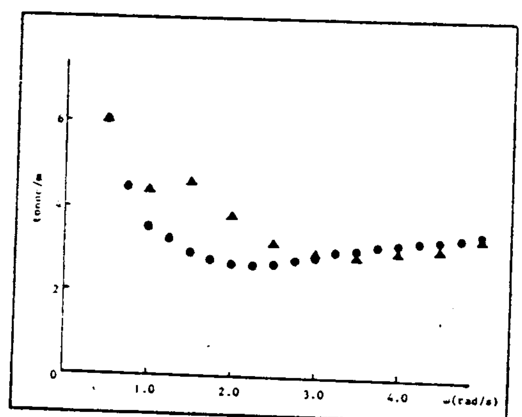

Figure V(g): Heave - Heave Added Mass.

Figure V(h): Heave - Heave Damping.

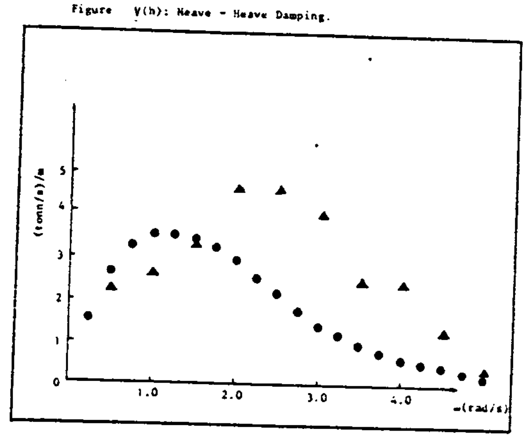

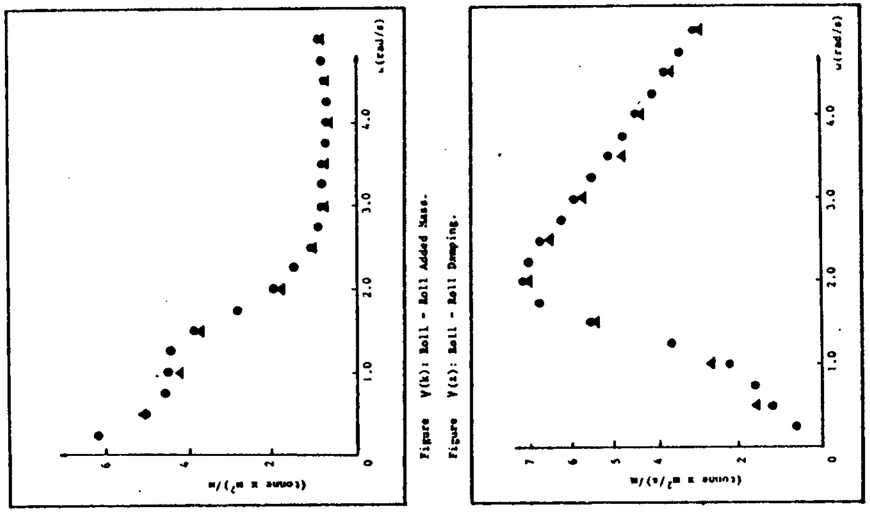

Figure V(k): Roll - Roll Added Mass.

Figure V(s): Roll - Roll Damping.

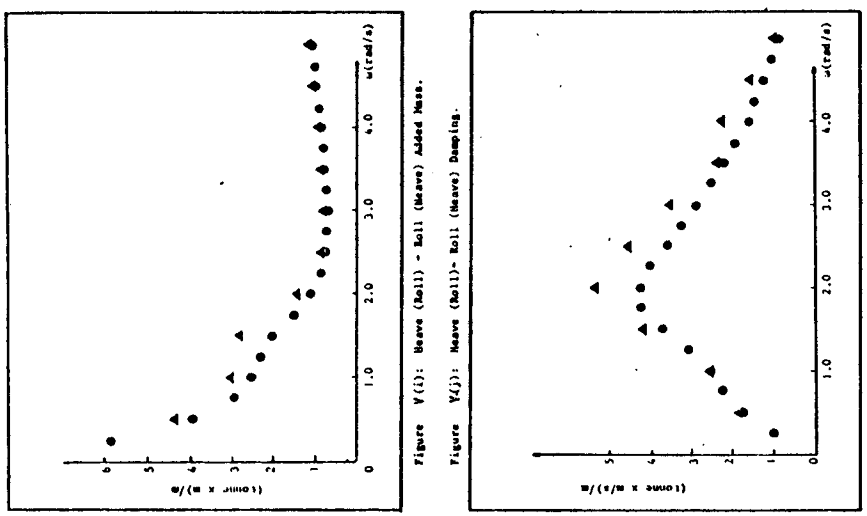

Figure V(i): Heave (Roll) - Roll (Heave) Added Mass.

Figure V(j): Heave (Roll)- Roll (Heave) Damping.

The responses to regular wave excitation of that beam were calculated considering beam sea ($\chi = 90^0$).

The following set of figures shows the amplitudes of the principal coordinates - $|p_r|$, r = 0, 2, 4, 5, 6, 7, when no allowance for structural damping is included.

SALTER'S DUCK RESPONSES IN REGULAR WAVES U = 0.00 m/sec. χ = 90.0 deg. a = 1.00 m

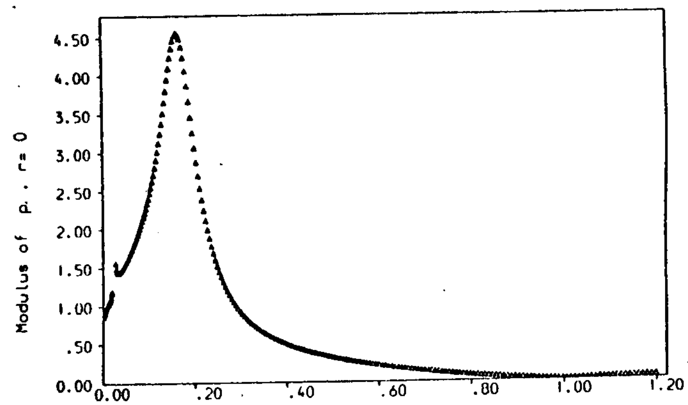

Figure VI(a)

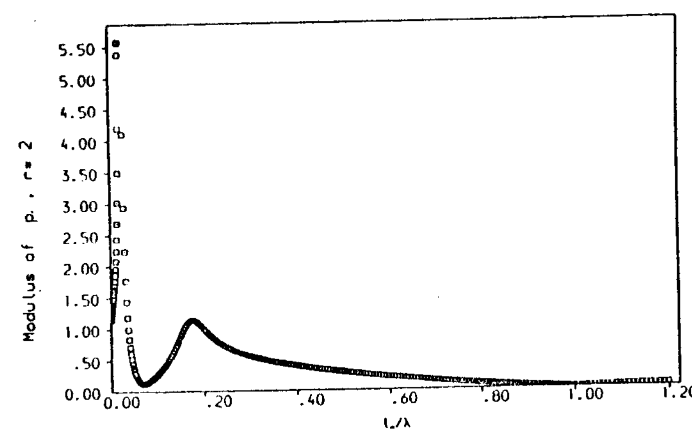

Figure VI(b)

SALTER'S DUCK RESPONSES IN REGULAR WAVES U = 0.00 m/sec.χ = 90.0 deg.a = 1.00 m

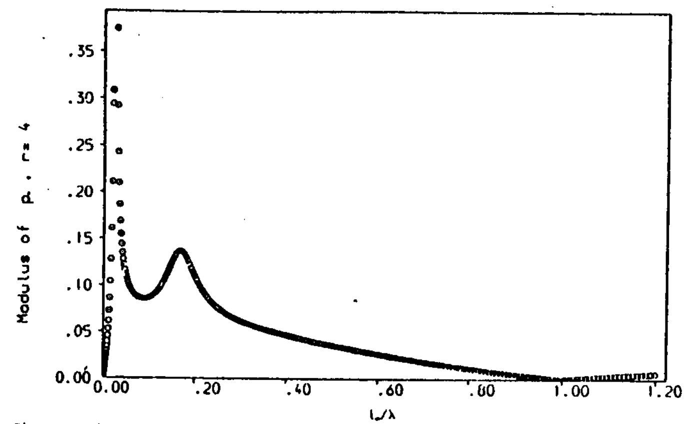

Figure VI(c)

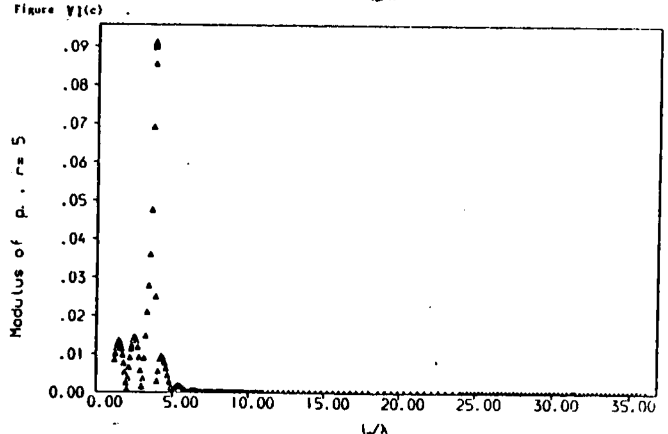

Figure VI(d)

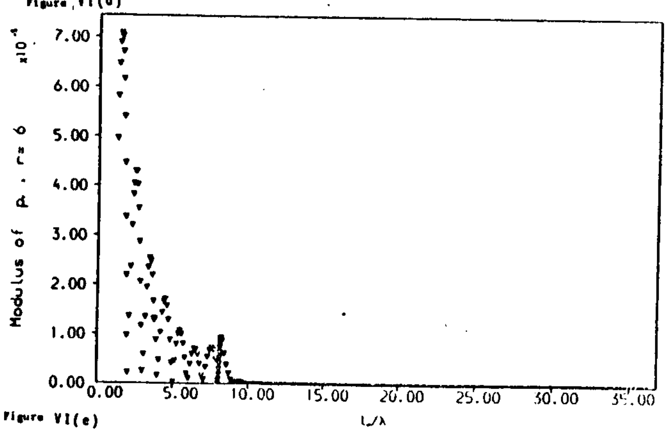

Figure VI(e)

SALTER'S DUCK RESPONSES IN REGULAR WAVES U = 0.00 m/sec.χ = 90.0 deg.a = 1.00 m

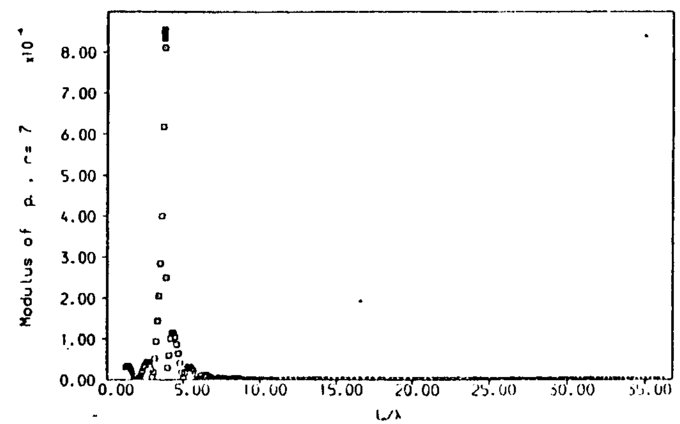

Figure VI(f)

As suggested by these curves, the order of magnitude of the responses at the rigid body motions (r = 0, 2 e 4) are much greater than those associated with distortions. The heave response - $|P_0|$ (Figure VI (a)) peaks at $\frac{\ell}{\lambda}$ = 0.162 (ω_e = 0.659 rad/s) corresponding to the resonance at natural frequency of heave. The roll response - $|P_4|$ (Figure VI (c)) peaks at $\frac{\ell}{\lambda}$ = 0.02 (ω_e = 0.23 rad/s) corresponding to the resonance at natural frequency of roll. Sway response - $|P_2|$ (Figure VI (b)) has peaks at these two values of $\frac{\ell}{\lambda}$ owing to coupling effects. The predominant value is located at $\frac{\ell}{\lambda}$ = 0.02, suggesting stronger coupling between sway and roll motions. As a consequence of the existing coupling between heave and roll, these responses have peaks at each other's natural frequencies (Figure VI(a) and (c)).

Furthermore, resonances associated with each value of the dry natural frequency should occur as well. As one would expect, at these resonant values corresponding response displays a peak. Table III presents the values of the resonant encounter frequency (and $\frac{\ell}{\lambda}$) corresponding to the four lowest distortional "dry"-natural frequencies of the Salter's Duck.

Mode	No. of nodes ℓ_x	ℓ_y	T	"dry" nat. frequency (rad/s)	Resonance (rad/s)	ℓ/λ
5	2	2	2	4.481	3.171	3.670
6	2	2	2	5.751	4.620	8.207
7	3	3	1	9.829	7.220	19.500
8	3	3	1	10.140	9.170	31.453

Table III: "Dry" and "wet" natural frequencies of the Salter's Duck ($\chi = 90°$, $\bar{U} = 0.0$ m/s). The Table shows the No. of nodes occurring in each mode shape and the dominant motions are underlined.

The following graphs complete the set of results showing the amplitudes of the bending moments and shear forces in both directions, and, the twisting moment, all taken at the most critical section of the Duck. These pictures allow the observation of the direct effect of the resonance upon the soliciting efforts acting on the Duck.

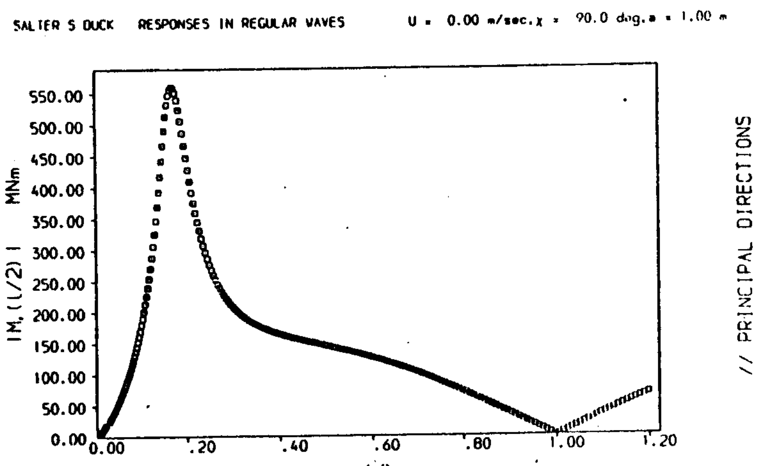

Figure VII(a)

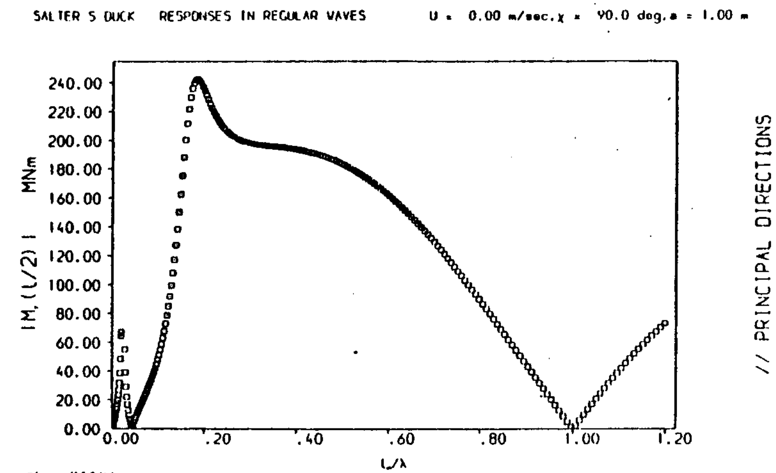

Figure VII(b)

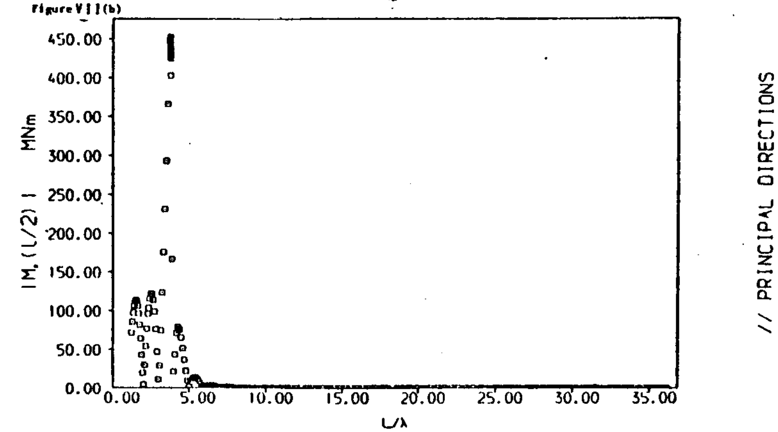

Figure VII(c)

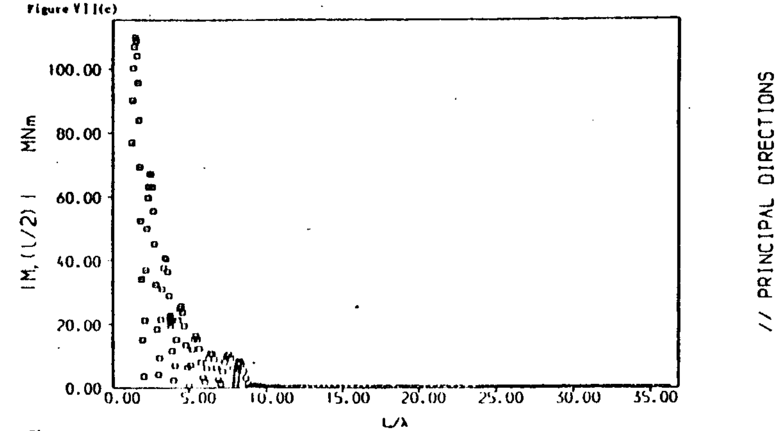

Figure VII(d)

SALTER S DUCK RESPONSES IN REGULAR WAVES U = 0.00 m/sec.χ = 90.0 deg.a = 1.00 m

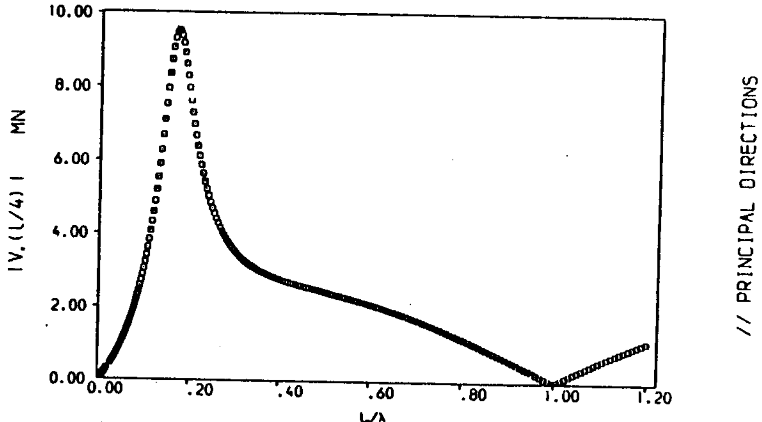

Figure VII(e)

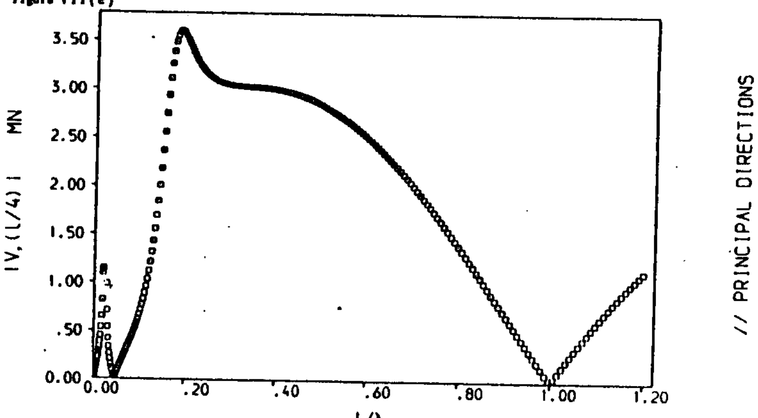

Figure VII(f)

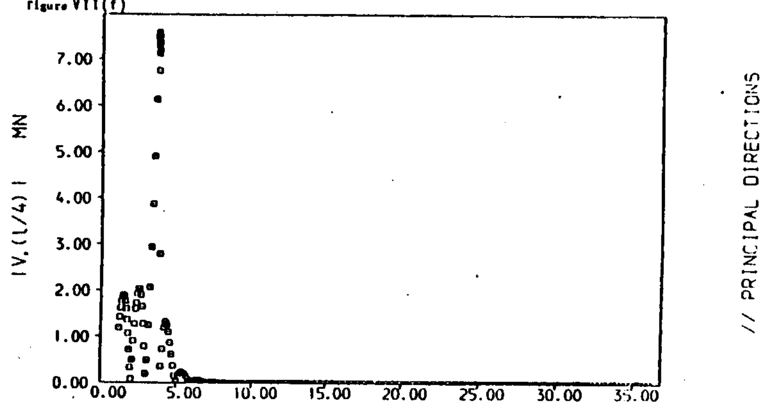

Figure VII(g)

SALTER S DUCK RESPONSES IN REGULAR WAVES U = 0.00 m/sec.χ = 90.0 deg.a = 1.00 m

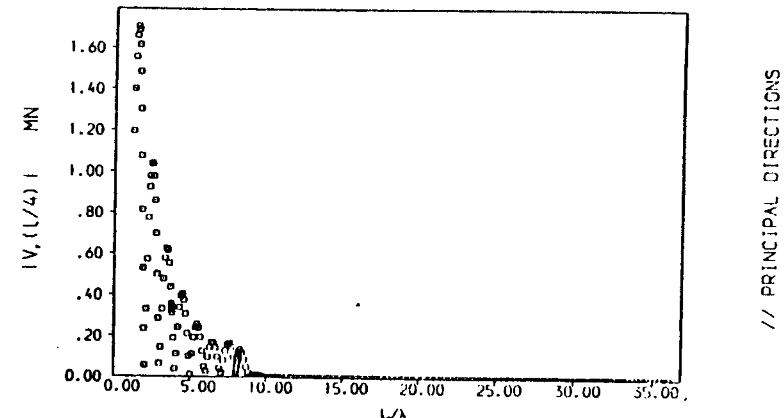

Figure VII(h)

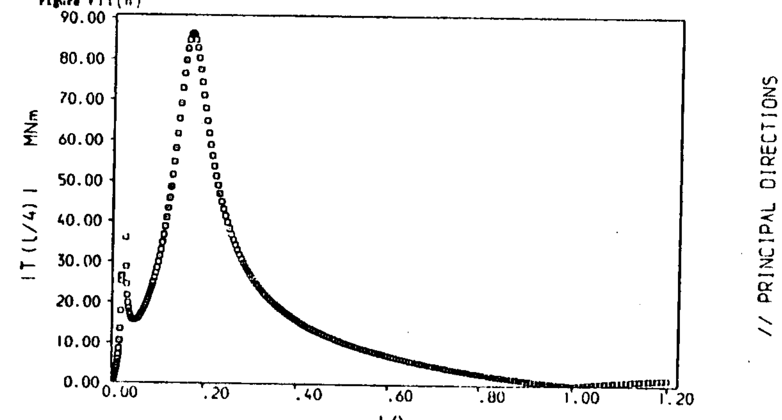

Figure VII(i)

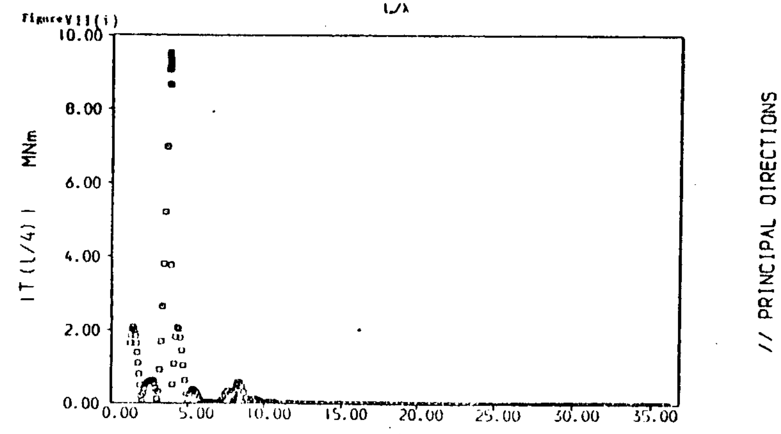

Figure VII(j)

IV - CONCLUSIONS

The technique presented here is a combination of linear structural dynamic with linear hydrodynamic theories, although non-linear hydrodynamic theory could be adapted if needed be.

The representation of the body as an elastic beam has proved to be accurate within certain limits (slender bodies oscillating at low frequencies as it is the case of the Salter's Duck) and makes the application of structural and hydrodynamic theories much easier.

Resonances at low frequencies, then, will be highly significant in determining the responses of a Salter's Duck Operating in a realistic seaway. Yet resonances at higher frequencies can also be of practical interest. In the analysis of long term statistics, hugh order moments of the spectral density function of the responses have to be taken into consideration. These moments act in order to magnify the contributions of even small peaks located at high values of frequency. Failure in predicting these resonances may produce rather inaccurate results.

The approach adopted in this work allows to reconcile in a single solution rigid body and distortional motions. The analysis demonstrated that whenever responses of unsymmetric bodies are concerned, they will be inevitably coupled in all three directions of motion.

BIBLIGRAPHY

1 - SALTER S.H.; JEFFREY D.C.; TAYLOR J.R.M.: The Architecture of Nodding Duck Wave Power Generators - The Naval Architect, Jan. 1976, England.

2 - EVANS D.V.; JEFFREY D.C.; SALTER S.H.; TAYLOR J.R.M.: Submerged Cylinder Wave Energy Device: Theory and Experiment - Applied Ocean Research, Vol. 1, No. 1, 1979.

3 - MINETT A.E.; SERMAN D.D.; MEI C.C.: Characteristics of Salter's Cam for Extracting Energy from Ocean Waves - Applied Ocean Research, Vol. 1, No. 1, 1979.

4 - KATORY M.; LACEY A.A.; TAM P.K.Y.: Application of Theoretical Hydrodynamics to the Design of Arbitrarily Shaped and Multi-bodied Marine Structures - RINA, 1979, England.

5 - KATORY, M.: Application of Theoretical Hydrodynamics to the Design of Wave Power Generators - The Naval Architect, May, 1976, England.

6 - KUMAI T.: Damping Factors in the Higher Modes of a Ship Vibration - European Shipbuilding 1, 1958.

7 - BETTS C.V.; BISHOP R.E.D.; PRICE W.G.: A Survey of Hull Damping - Trans. RINA, 119, 1977, England.

8 - TIMOSHENKO S.P.: Strength of Materials - Part II - Advanced Theory and Problems, 3rd edition, 1956, D.van Nostrand Co..

9 - HASLÜM K.; TONNESSEN A.: An Analysis of Torsion in Ship Hulls, European Shipbuilding No. 5/6, 1972.

10 - BISHOP R.E.D.; PRICE W.G.: Hydroelasticity of Ships - 1979, Cambridge University Press.

11 - CONCEIÇÃO C.A.L.: Responses of Flexible Unsymmetric Bodies in Waves - Ph.D. Thesis - University of London, 1981.

12 - BISHOP R.E.D.; CONCEIÇÃO C.; PRICE W.G.: The Influence of Unsymmetric Hull Form on the Heave, Sway and Roll Hydrodynamic Coefficients - SOBENA, 1980, BRAZIL.